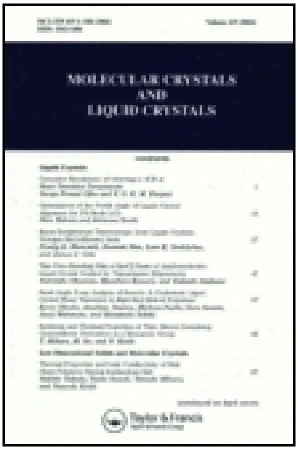

Molecular Crystals and Liquid Crystals Incorporating Nonlinear Optics
Publication details, including instructions for authors and subscription information:
http://www.tandfonline.com/loi/gmcl17

Retro-Self-Focusing and Pinholing Effect in a Cholesteric Liquid Crystal

Jae-Cheul Lee [a], Stephen D. Jacobs [a] & Ansgar Schmid [a]
[a] Laboratory for Laser Energetics, University of Rochester, 250 East River Road, Rochester, NY, 14623-1299
Version of record first published: 13 Dec 2006.

To cite this article: Jae-Cheul Lee , Stephen D. Jacobs & Ansgar Schmid (1987): Retro-Self-Focusing and Pinholing Effect in a Cholesteric Liquid Crystal, Molecular Crystals and Liquid Crystals Incorporating Nonlinear Optics, 150:1, 617-629

To link to this article: http://dx.doi.org/10.1080/00268948708074819

Mol. Cryst. Liq. Cryst., 1987, Vol. 150b, pp. 617–629
Photocopying permitted by license only

Printed in the United States of America

Retro-Self-Focusing and Pinholing Effect in a Cholesteric Liquid Crystal

JAE-CHEUL LEE, STEPHEN D. JACOBS and ANSGAR SCHMID

Laboratory for Laser Energetics, University of Rochester, 250 East River Road, Rochester, NY 14623-1299

(*Received July 15, 1987*)

In this paper, we show theoretically that a cholesteric liquid crystal exhibits a retro-self-focusing effect and a pinholing effect under the Gaussian intensity distribution of an incident optical field. The retro-self-focusing effect is a result of pitch dilation due to intense optical radiation. We confirm these theoretical predictions by experiment.

INTRODUCTION

The cholesteric class of liquid crystals (CLC) has several properties which are important for laser applications. These properties are high optical rotatory power and circular dichroism. As is well known, the CLC structure has an anomalously high optical activity by which the rotation of the plane of polarization of optical radiation may reach several thousands of degrees per millimeter. It also exhibits a form of the circular dichroism in which one circularly polarized component is reflected and the other transmitted. The reflected light is circularly polarized with the same sense of handedness as the incident light. Applications[1,2] using these properties include polarizers, bandpass and notch filters, mirrors, apodizers and optical isolators to prevent back reflections in laser systems. These are all based on the linear propagation of light through the medium. But in intense optical fields, nonlinear effects can occur. For such conditions, H. G. Winful[3] solved the coupled Euler-Lagrange and Maxwell equations to show bistability in the CLC class due to a light-induced pitch change of the cholesteric helix.

In this paper we will show theoretically that the CLC structure also has a retro-self-focusing effect under exposure to a plane wave with a Gaussian intensity distribution. Specifically, the reflected field comes to a focus due to intensity dependent phase modulation. We will also derive equations to describe a pinholing effect. Experimental results will be offered in support of the theoretical predictions.

THEORY

For convenience, we will rewrite and rederive some of Winful's equations. Let us consider a right-handed CLC cell as shown in Fig. 1 whose helix axis is oriented along the z-axis. The helical structure of the CLC can be described by the director $\hat{n}(z)$ which represents the average orientation of the elongated liquid-crystal molecules. As shown in Figure 1, the pitch is the distance required for the director to rotate by 360°. Its cartesian components are:

$$n_x = \cos\theta(z),\ n_y = \sin\theta(z),\ n_z = 0 \tag{1}$$

In the absence of external fields, the angle $\theta(z)$ is given by $\theta = q_0 z$, where q_0 is the unperturbed wave number of the helix whose pitch is $p_0 = 2\pi/q_0$.

When right circularly polarized light propagates along the z-axis, the total electric field E in the medium can be described by circularly polarized components as follows:

$$\mathbf{E} = \mathrm{Re}\{E_+(z)(\hat{x} - i\hat{y})/\sqrt{2} + E_-(z)(\hat{x} + i\hat{y})/\sqrt{2}\}e^{-i\omega t} \tag{2}$$

where $E_\pm = (E_x \pm E_y)/\sqrt{2}$. The first term in Eq. (2) represents a forward-propagating wave and the second term represents a counter-propagating wave which has the same sense of polarization as the forward-propagating wave. The free energy density F per unit volume of material under the influence of the electric field E is taken in the form[4]

$$F = \frac{1}{2}k_{11}(\nabla \cdot \hat{n})^2 + \frac{1}{2}k_{22}(\hat{n} \cdot \nabla \times \hat{n} + q_0)^2 + \frac{1}{2}k_{33}(\hat{n} \times \nabla \times \hat{n})^2 - \mathbf{E} \cdot \mathbf{D}/8\pi \tag{3}$$

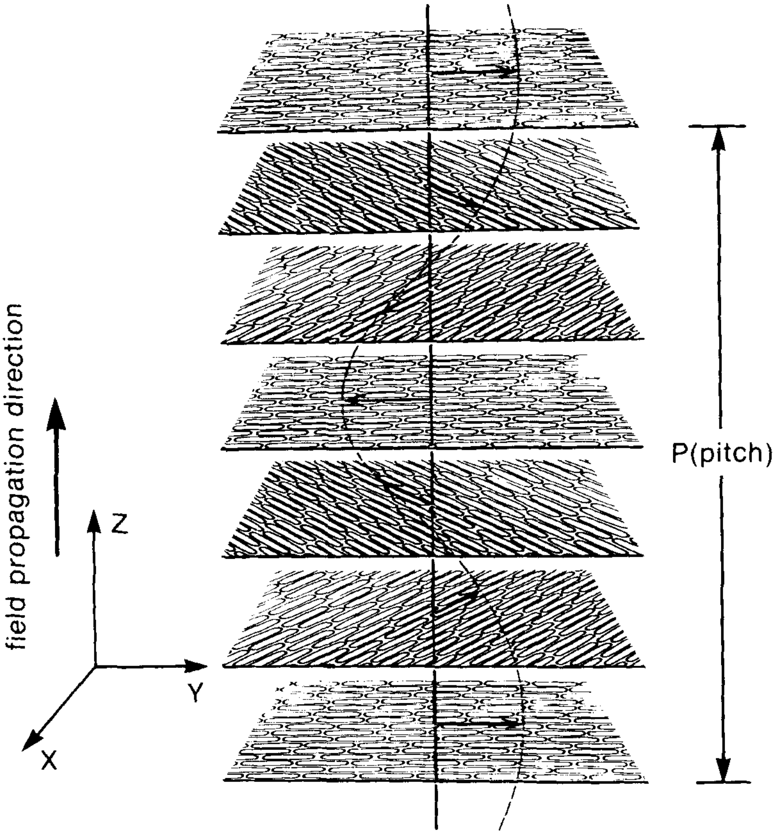

FIGURE 1 Schematic diagram of a cholesteric liquid crystal.

where k_{11}, k_{22}, k_{33} are the Frank elastic constants in units of dynes, $\mathbf{D} = \epsilon_{\perp}\mathbf{E} + \epsilon_a\hat{n}(\hat{n} \cdot \mathbf{E})$, $\epsilon_a = \epsilon_{\parallel} - \epsilon_{\perp}$ and where ϵ_a is the optical dielectric anisotropy and $\epsilon_{\parallel}$ and $\epsilon_{\perp}$ represent the dielectric constants parallel and perpendicular to the local director. In the case of a CLC which has a planar structure with the component of the director as described in Eq. (1), the first and third terms in Eq. (3) disappear and only the second term remains. The new configuration of the director due to the electric field **E** can be found by minimizing the free energy density F. This leads to the Euler Lagrange equation:

$$\frac{d^2\theta}{dz^2} = \frac{\epsilon_a}{8\pi k_{22}} [\mathrm{Re}(E_+ E_-^*)\, sin2\theta - \mathrm{Im}(E_+ E_-^*)\, cos2\theta] \qquad (4)$$

where $\theta(z)$ is the perturbed director angle. Maxwell's equation in the medium can be rewritten as

$$-\frac{d^2E_\pm}{dz^2} = k_0^2E_\pm + k_1^2E_\mp e^{\pm i2\theta} \tag{5}$$

where $k_0^2 = (\omega/c)^2(\in_\| + \in_\perp)/2$ and $k_1^2 = (\omega/c)^2\in_a/2$. As a trial solution, the forward-propagating wave and counter-propagating wave in the medium can be represented as

$$E_\pm = |\epsilon_\pm(z)| \exp[i\phi_\pm(z) \pm iq_0z] \tag{6}$$

By substituting Eq. (6) into Eq. (5), Maxwell's equation can be rewritten as a coupled amplitude equation in a slowly varying envelope approximation.

$$\frac{d|\epsilon_+|}{dz} = \kappa|\epsilon_-| \sin\Psi \tag{7}$$

$$\frac{d|\epsilon_-|}{dz} = \kappa|\epsilon_+| \sin\Psi \tag{8}$$

$$\frac{d\Psi}{dz} = 2(q_0 + \Delta k) + \kappa(|\epsilon_-|/|\epsilon_+| + |\epsilon_+|/|\epsilon_-|) \cos\Psi - 2\frac{d\theta}{dz} \tag{9}$$

where $\Psi = \phi_+ - \phi_- + 2q_0z - 2\theta$, $\kappa = k_1^2/2q_0$, and $\Delta k = (k_0^2 - q_0^2)/2q_0$. At this point, boundary conditions are introduced for a CLC with strong surface anchoring at $z = 0$ and no surface anchoring at $z = L$ (where L is the total CLC fluid thickness):

$$|\epsilon_+(L)| = |\epsilon_T|, \quad \text{the transmitted field at } z = L \tag{10}$$

$$|\epsilon_-(L)| = 0, \quad \text{no reflection at } z = L \tag{11}$$

$$\left.\frac{d\theta}{dz}\right|_{z=L} = q_0, \quad \text{no anchoring at } z = L \tag{12}$$

$$\theta(0) = 0, \quad \text{strong anchoring at } z = 0 \tag{13}$$

Substituting Eq. (6) into (4), yields the dependence of the director angle on the forward-propagating intensity.

$$\frac{d^2\theta}{dz^2} = \frac{-\in_a}{16\pi k_{22}\kappa}\frac{d|\epsilon_+|^2}{dz} \tag{14}$$

Integration of Eq. (14) with boundary condition Eq. (12), gives

$$q(z) = \frac{d\theta}{dz} = q_0 - \frac{\in_a}{16\pi k_{22}\kappa}(|\epsilon_+(z)|^2 - |\epsilon_T|^2) \tag{15}$$

The last expression shows that $q(z) \leq q_0$. Therefore the pitch will increase or dilate in proportion to the optical field intensity ($|\epsilon_+(z)|^2$) along the z-axis by $p = 2\pi/q$. The maximum dilation occurs around $z = 0$. From Eq. (2), (4), (5), and (15), we find

$$\frac{d}{dz}(|\epsilon_+\epsilon_-|\cos\Psi) = -\frac{1}{\kappa}\frac{d|\epsilon_+|^2}{dz}\left[\Delta k + \frac{\in_a}{16\pi k_{22}\kappa}(|\epsilon_+|^2 - |\epsilon_T|^2)\right] \tag{16}$$

Let $u(z) = \gamma|\epsilon_+(z)|^2$, $J = \gamma|\epsilon_T|^2$ and $v(z) = \gamma|\epsilon_-(z)|^2$, where $\gamma = \in_a/32\pi k_{22}\kappa^2$.

Rewriting Eq. (16), we have

$$\frac{d}{dz}\sqrt{uv}\cos\Psi = -\left[\frac{\Delta k}{\kappa} + 2(u - J)\right]\frac{du}{dz} \tag{17}$$

Integrating Eq. (17) with respect to z gives

$$\sqrt{uv}\cos\Psi = -(\Delta k/\kappa - 2J)u - u^2 + C$$

Where C is a constant of integration. From the boundary condition, Eq. (10) and Eq. (11), $u(L) = J$ and $v(L) = 0$ respectively, and the solution for Eq. (17) takes the form

$$\sqrt{uv}\cos\Psi = -(u - J)[\Delta k/\kappa + (u - J)] \tag{18}$$

Since $d|\epsilon_+|/dz < 0$ in Eq. (7), $\sin\Psi < 0$.

Therefore Eq. (18) becomes

$$\sqrt{uv}\sin\Psi = -[(u - J)\{u - (u - J)[\Delta k/\kappa + (u - J)]^2\}]^{1/2} \tag{19}$$

$$\sin\Psi = -[1 - (1 - J/u)\{\Delta k/\kappa + (u - J)\}^2]^{1/2} \tag{20}$$

If we now multiply Eq. (7) by $|\epsilon_+|$ and rearrange it, we have

$$\frac{d}{dz}|\epsilon_+|^2 = 2\kappa|\epsilon_+\epsilon_-|\sin\Psi \tag{21}$$

Substituting Eq. (19) into Eq. (21), one finds

$$\begin{aligned}\frac{du}{dz} &= -2\kappa[(u-J)\{u-(u-J)[\Delta k/\kappa + (u-J)]^2\}]^{1/2} \\ &= -2\kappa[Q(u)]^{1/2}\end{aligned} \tag{22}$$

where $Q(u) = (u - J)\{u - (u - J)(\Delta k/\kappa + u - J)^2\}$

When the roots of $Q(u)$ are real and $u_1 > u_2 > u_3 > u_4$, Eq. (22) may be solved in terms of a Jacobian elliptic function

$$u(z) = u_3 + \frac{u_2 - u_3}{1 - (u_1 - u_2)(u_1 - u_3)^{-1} Sn^2[2\kappa(z - L)/g, k]} \tag{23}$$

where Sn is a Jacobian elliptic function with $g = 2/[(u_1 - u_3)(u_2 - u_4)]^{1/2}$ and $k = [(u_1 - u_2)(u_3 - u_4)]^{1/2} g/2$. When the two roots of $Q(u)$ are real and $u_1 \geq u \geq u_2$ and the two roots u_3 and u_4 are complex, the solution of Eq. (22) becomes

$$u(z) = \frac{Bu_1 + Au_2 + (Au_2 - Bu_1)Cn[2\kappa(z - L)/g, k]}{A + B + (A - B)Cn[2\kappa(z - L)/g, k]} \tag{24}$$

where $A^2 = (u_1 - b_1)^2 + b_2^2$, $B^2 = (u_2 - b_1)^2 + b_2^2$, $b_1 = \mathrm{Re}[u_3]$ and $b_2 = \mathrm{Imag}[u_3]$, and Cn is a Jacobian elliptic function with $g = 1/\sqrt{AB}$ and $b_2 = \{(u_1 - u_2)^2 - (A - B)^2\}/4AB$.

A plot of the normalized intensity $u(z)$ for the forward-propagating wave and $v(z)$ for the counter-propagating wave in the CLC medium is shown in Figure 2. The incident field intensity $u(z)$ decays almost exponentially along the z-axis. This decay, however, is due to energy transfer to the counter-propagating field, and not due to absorption. The relationship between incident field intensity I at $z = 0$ and transmitted field intensity J at $z = L$ for $\kappa L = 2$ with $\Delta k/\kappa = 0$, ± 0.1 is shown in Figure 3. As H. G. Winful has already shown, optical bistability is predicted. Higher ($\Delta k/\kappa < 0$) and lower ($\Delta k/\kappa > 0$) intensities are required for a discontinuous jump in comparison to the case where $\Delta k/\kappa = 0$. Physically, $\Delta k/\kappa = 0$ means that the pitch of a CLC is exactly Bragg-matched to the wavelength of an incident

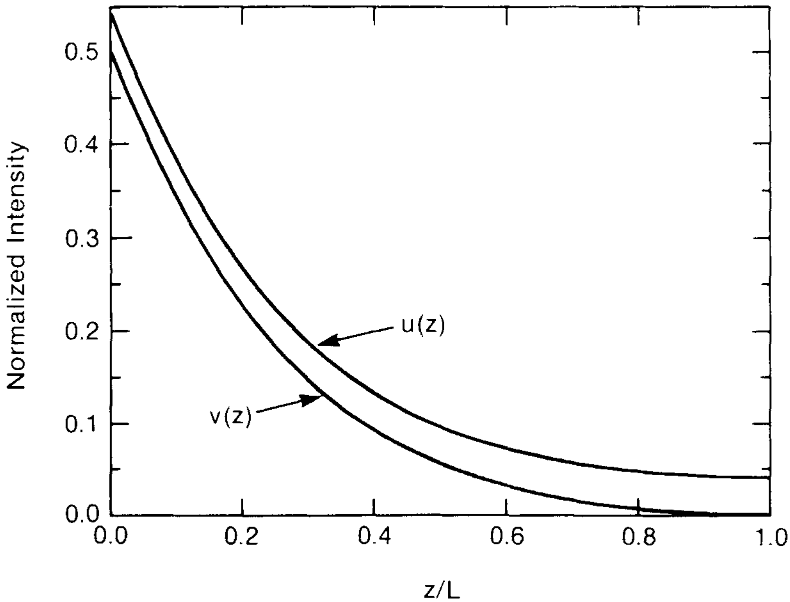

FIGURE 2 Normalized forward propagating field intensity $u(z)$ and counter propagating field intensity $v(z)$ through the medium, for $\kappa L = 2.0$.

field by the Bragg (selective) reflection condition $\lambda_0 = n_{av} \cdot p_0$ where λ_0 is the wavelength of selective reflection, n_{av} average refractive index for liquid crystal and p_0 is the pitch of CLC structure.

Now let us calculate the phase $\phi_-(z)$ of the reflected wave at $z = 0$. At $z = 0$, $\Psi = \phi_+(0) - \phi_-(0)$. From Eq. (18),

$$\phi_-(0) = \phi_+(0) - \cos^{-1}[-\sqrt{1 - J/I}\{\Delta k/\kappa + (I - J)\}] \quad (25)$$

where $I = u(0)$. Equation (25) shows explicitly the intensity dependence of the phase shift. Figure 4 shows the phase of the reflected wave as a function of normalized input intensity and the detuning parameter $\Delta k/\kappa$ when $\phi_+(0) = 0$. When $\Delta k/\kappa = 0$, the intense field destroys the Bragg condition $\lambda_0 = n_{av} \cdot p_0$ and the phase linearly decreases from 90° as the input field intensity increases. Note the 90° phase difference between the incident and reflected fields near zero intensity. This comes from the mathematical representation of the reflected field in Eq. (2). There we used $E_-(z)(\hat{x} + i\hat{y})/\sqrt{2}$ to describe the reflected field which is right circularly polarized. When $\Delta k/\kappa < 0$, the pitch dilates as the input intensity increases, and at a certain intensity the incident field satisfies the Bragg condition. In Figure 4,

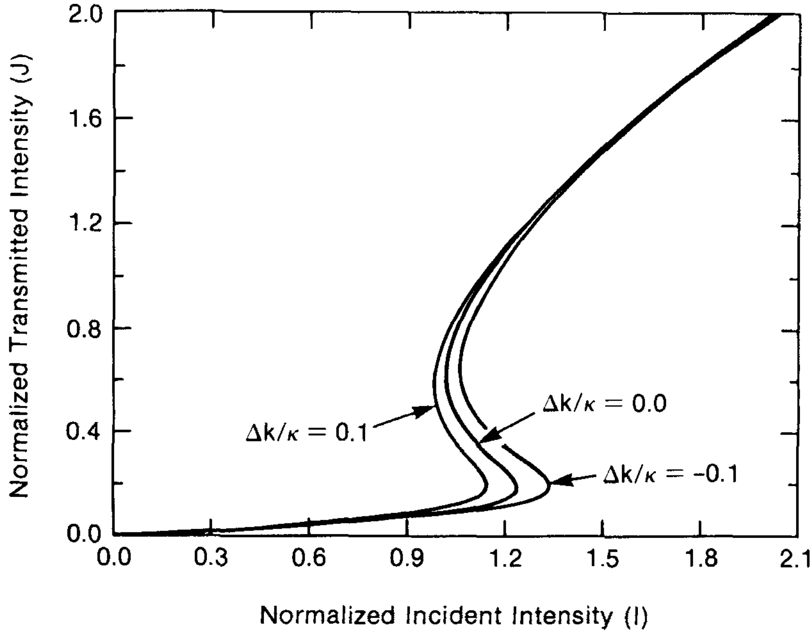

FIGURE 3 Transmitted intensity vs incident intensity for $\kappa L = 2.0$ for various values of the detuning parameter $\Delta k/\kappa = 0, \pm 0.1$). Intensities are normalized by $32\pi k_{22}\kappa^2/\epsilon_a$.

when $\Delta k/\kappa = -0.1$, the phase of the reflected field increases with intensity from ~83° to 90° where the Bragg condition is met. The phase then decreases for higher intensity levels. When $\Delta k/\kappa > 0$, the pitch of the CLC is already out of the Bragg condition. Its initial phase is less than 90° and it decreases with increasing intensity. The physical origin of this intensity dependence of the phase of a reflected field is as follows: higher field intensities cause a larger pitch dilation ($\epsilon_a > 0$). As a result, the Bragg reflection condition is perturbed and the optical field penetrates more deeply into the CLC before being reflected.

A very interesting condition results from considering a plane wave with intensity distribution $I_p(x, y) = |E(x, y)|^2$ incident on the CLC. Consider the case where $E(x, y)$ is a Gaussian distribution of the intensity in Eq. (26).

$$I_p(r) = \left| E_0 \exp\left[-\frac{r^2}{w^2} \right] \right|^2 = I_0 \exp\left[-\frac{2r^2}{w^2} \right] \tag{26}$$

where w is the spot size of the beam. Rewriting this as a normalized

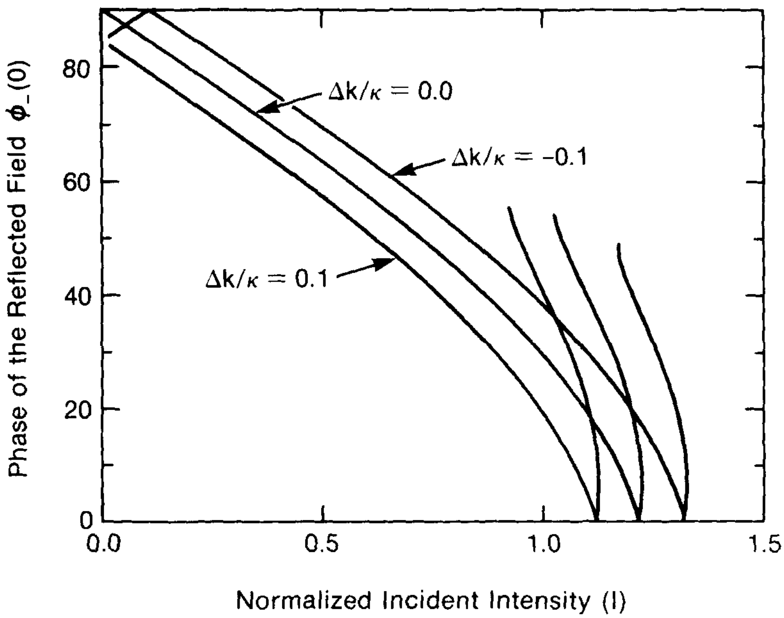

FIGURE 4 Incident field intensity vs the phase of the reflected field when the phase of the incident field $\phi_+(0) = 0$. (For $\kappa L = 2.0$ and for various values of the detunig parameter $\Delta k/\kappa = 0, \pm 0.1$).

intensity with γ and introducing a radial-dependence, one finds

$$u = \gamma |E(r,z)|^2$$
$$u(0) = I = \gamma |E(r,o)|^2 = \gamma |E_0|^2 \exp\left(-\frac{2r^2}{w^2}\right) \quad (27)$$

By substituting Eq. (27) into Eq. (25), one derives the transverse phase shift of the reflected wave due to a Gaussian intensity distribution. In the first approximation, it is assumed that the first and third terms in Eq. (3) are still negligible. For $I >> J$, i.e., for the lower-branch condition in the bistability curve of Figure 3, Eq. (25) reduces to

$$\cos\phi_-(0) = -\{\Delta k/\kappa + I\}$$
$$= -\left\{\Delta k/\kappa + \gamma |E_0|^2 \exp\left[-\frac{2r^2}{w^2}\right]\right\} \quad (28)$$
$$\cong 1 - \frac{\phi_-^2(0)}{2!} [\phi_-(0) \lesssim \pi/4]$$

One can now readily derive the phase distribution of the reflected field,

$$\phi_{-}(0) = [2(1 + \Delta k/\kappa)]^{1/2}\left[1 + \frac{\gamma|E_0|^2 \exp\left\{\frac{-2r^2}{w^2}\right\}}{2(1 - \Delta k/\kappa)}\right] \quad (29)$$

Under the Bragg condition $\Delta k/\kappa = 0$, Eq. (29) becomes

$$\phi_{-}(0) \cong \sqrt{2}\left(1 + \frac{\gamma|E_0|^2}{2}\right) - \frac{\sqrt{2}\gamma|E_0|^2 r^2}{w^2} + \frac{2\sqrt{2}\gamma|E_0|^2 r^4}{w^4} \quad (30)$$

The first term of Eq. (30) corresponds to the constant phase change. The second term corresponds to the quadratic phase change, and the third term corresponds to a spherical aberration (r^4 dependence). Note that $\phi_{-}(0)$ is almost constant when $|r| > w/\sqrt{2}$. Therefore, any retro-self-focusing effect can only occur within $|r| \leq w/\sqrt{2}$. This can be interpreted as a form of pinholing or apodizing effect where the aperture possesses a soft edge. By analogy with the quadratic phase term of a Gaussian beam, we can calculate the intensity dependent radius of curvature of the reflected field as

$$R = \frac{-\pi w^2}{\lambda}\frac{1}{\sqrt{2}\gamma|E_0|^2} \quad (31)$$

Equation (31) indicates a retro-self-focusing effect because the radius of curvature is negative and inversely proportional to the intensity as we expect.

EXPERIMENT

Retro-self-focusing and the pinholing effects have been observed in an experiment using a CLC-dielectric resonator as shown in Figure 5. This CLC-dielectric resonator consists of flat dielectric HR end

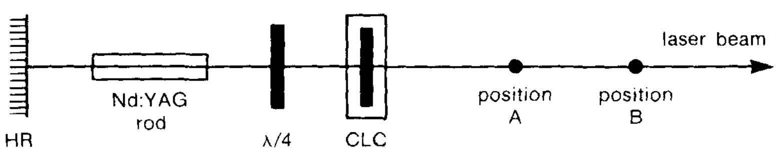

FIGURE 5 Schematic diagram for experimental set-up (HR: high reflectivity flat dielectric mirror, $\lambda/4$: uncoated quarter wave plate, CLC: flat cholesteric liquid crystal mirror.)

mirror, a Nd:YAG laser rod, a λ/4 plate, and a CLC end mirror. Flat-flat substrates are used to make a CLC end mirror with a planar texture. We used a commercial Nd:YAG laser with the output coupler replaced by the CLC mirror. Light between the λ/4 plate and the dielectric mirror is linearly polarized, whereas the light between the λ/4 plate and the CLC mirror is circularly polarized. The output beam coupling comes from the Fresnel reflections off the uncoated wave-plate surfaces. The reflected light from the CLC mirror does not experience a 180° phase shift as is the case for reflection from a conventional mirror. The light reflected from the λ/4 plate, however, does experience a 180° phase shift and is coupled out of the cavity through the CLC mirror without experiencing selective reflection. Without a λ/4 plate, lasing does not occur in this configuration, because the conventional reflection from the dielectric HR mirror permits 100% transmission through the CLC mirror after every bounce.

The CLC-dielectric resonator was compared with dielectric flat-flat and dielectric flat-concave resonator configurations. The flat-flat configuration was very sensitive to the alignment of the mirrors ($\sim \pm 0.8$ arcsec). In contrast, the CLC-dielectric resonator was quite tolerant to misalignment ($\sim \pm 1.8$ arcsec). The CLC mirror acts as a concave mirror with an angular sensitivity which is the same as that of the dielectric flat-concave (5M radius curvature) resonator. The diameter of the output beam for the CLC-dielectric resonator was measured at two different position A and B as indicated in Figure 5. The beam diameter at the position A as observed by a 2-dimensional CID camera[5] was 10% greater than the beam size at the position B. This means that although the CLC end mirror (planar texture) was made from flat-flat substrates, it acts as a concave mirror. This is strong evidence for the CLC retro-self-focusing effect. In addition, the output beam exhibited an excellent Gaussian-mode as a result of the pinholing effect from the CLC mirror. The mode from the dielectric flat-flat resonator was TEM_{10} unless a hard edged pinhole was inserted. The output of CLC-dielectric cavity is shown in Figure 6. Figure 6 is slightly exaggerated at the center to make the solid lines and the dotted lines distinguishable. Further details of the experiment will be described elsewhere.[6]

CONCLUSION

We have shown theoretically that in the presence of intense optical radiation with a Gaussian beam profile, the CLC structure has a retro-

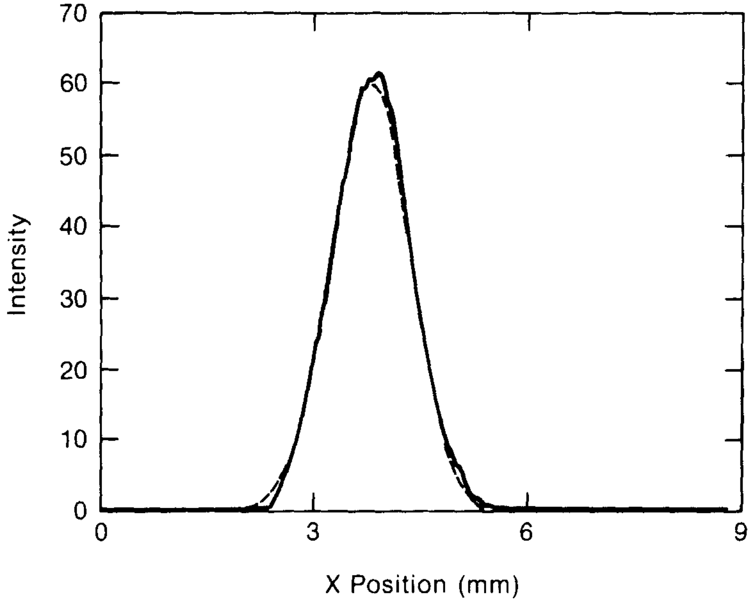

FIGURE 6 Output beam intensity distribution at position A (solid lines: Real output beam intensity, dotted lines: Ideal Gaussian beam intensity distribution). The numbers in the ordinate represent digital counts.

self-focusing effect and a pinholing effect. The ease of alignment for a CLC-dielectric resonator and the angular insensitivity of a CLC mirror which we observe experimentally result from the retro-self-focusing effect of the CLC mirror. The TEM_{00} mode structure which occurs without any physical hard aperture internal to the CLC-dielectric resonator results from the pinholing effect which occurs over the central region ($r \leq w/\sqrt{2}$.) of the Gaussian beam. Retro-self-focusing effects are a result of pitch dilation due to the nonlinear coupling of the intense optical field with the CLC helix structure. We are presently conducting a more detailed investigation of CLC mirrors in different resonator configurations.

Acknowledgments

The authors gratefully acknowledge H. G. Winful, R. W. Boyd, J. Kelly, Jim Walker and R. G. Lyon for valuable discussions, K. Marshall for help in fabricating cholesteric liquid crystals, and W. Castle for discussions on experimental technique.

This work was supported in part by Daewoo Heavy Industries, Ltd., of Incheon, Korea, the U.S. Department of Energy Office of Inertial Fusion under agreement No.

DE-FC08-85DP40200, the New York State Center for Advanced Optical Technology (NYSCAOT) of The Institute of Optics and by the Laser Fusion Feasibility Project at the Laboratory for Laser Energetics which has the following sponsors: Empire State Electric Energy Research Corporation, General Electric Company, New York State Energy Research and Development Authority, Ontario Hydro, and the University of Rochester. Such support does not imply endorsement of the content by any of the above parties.

References

1. S. D. Jacobs, "Liquid Crystals for Laser Applications," *Handbook of Laser Science and Technology*, edited by M. J. Weber, Vol. IV, Part 2 (CRC Press, Boca Raton, FL, 1986), pp. 409–465.
2. S. D. Jacobs, K. A. Cerqua, K. M. Marshall, T. J. Kessler, R. J. Gingold, P. J. Laverty and M. Topp, "High Power Laser Beam Apodization Using a Liquid Crystal Soft Aperture," Technical Digest-CLEO '86, THG_2, pp. 258–259, San Francisco, CA (June 1986).
3. Herbert G. Winful, "Nonlinear Reflection in Cholesteric Liquid Crystals: Mirrorless Optical Bistability," *Phys. Rev. Lett.*, **49**, 1179–1182 (1982).
4. P. G. de Gennes, "The Physics of Liquid Crystals" (Clarendon, Oxford, 1974), p. 243.
5. GE model TN 2505, array size: 248 V $\times$ 388 H pixels, pixel size: 27.3 μm $\times$ 23.3 μm.
6. J. C. Lee, S. D. Jacobs and R. J. Gingold, "Nd:YAG Laser with Cholesteric Liquid Crystal Cavity Mirrors," presented at the 31st SPIE Annual International Technical Symposium, San Diego, CA, 16–21 August 1987 (Vol. 824).